Identification of Differential Transcriptional Patterns in Primary and Secondary Hyperparathyroidism

Samira Mercedes Sadowski,[1] Marc Pusztaszeri,[2,3] Marie-Claude Brulhart-Meynet,[4,5] Volodymyr Petrenko,[4,5,6,7] Claudio De Vito,[2] Jonathan Sobel,[8] Céline Delucinge-Vivier,[6] Electron Kebebew,[9] Romano Regazzi,[8] Jacques Philippe,[4,5] Frédéric Triponez,[1] and Charna Dibner[4,5,6,7]

[1]Department of Thoracic and Endocrine Surgery, University Hospitals of Geneva and Faculty of Medicine, University of Geneva, Geneva 1211, Switzerland; [2]Division of Clinical Pathology, University Hospitals of Geneva, Geneva 1211, Switzerland; [3]Department of Pathology, Jewish General Hospital and McGill University, Montreal H3A2B4, Canada; [4]Division of Endocrinology, Diabetes, Hypertension and Nutrition, University Hospitals of Geneva, Geneva 1211, Switzerland; [5]Diabetes Centre, Faculty of Medicine, University of Geneva, Geneva 1211, Switzerland; [6]iGE3 Genomics Platform, University of Geneva, Geneva 1211, Switzerland; [7]Department of Cell Physiology and Metabolism; Faculty of Medicine, University of Geneva, Geneva 1211, Switzerland; [8]Department of Fundamental Neurosciences, University of Lausanne, Lausanne 1005, Switzerland; and [9]Department of Surgery, Stanford University, California 94305

Context: Hyperparathyroidism is associated with hypercalcemia and the excess of parathyroid hormone secretion; however, the alterations in molecular pattern of functional genes during parathyroid tumorigenesis have not been unraveled. We aimed at establishing transcriptional patterns of normal and pathological parathyroid glands (PGs) in sporadic primary (HPT1) and secondary hyperparathyroidism (HPT2).

Objective: To evaluate dynamic alterations in molecular patterns as a function of the type of PG pathology, a comparative transcript analysis was conducted in subgroups of healthy samples, sporadic HPT1 adenoma and hyperplasia, and HPT2.

Design: Normal, adenomatous, HPT1, and HPT2 hyperplastic PG formalin-fixed paraffin-embedded samples were subjected to NanoString analysis. *In silico* microRNA (miRNA) analyses and messenger RNA–miRNA network in PG pathologies were conducted. Individual messenger RNA and miRNA levels were assessed in snap-frozen PG samples.

Results: The expression levels of *c-MET, MYC, TIMP1*, and clock genes *NFIL3* and *PER1* were significantly altered in HPT1 adenoma compared with normal PG tissue when assessed by NanoString and quantitative reverse transcription polymerase chain reaction. *RET* was affected in HPT1 hyperplasia, whereas *CaSR* and *VDR* transcripts were downregulated in HPT2 hyperplastic PG tissue. *CDH1, c-MET*, *MYC*, and *CaSR* were altered in adenoma compared with hyperplasia. Correlation analyses suggest that *c-MET, MYC*, and *NFIL3* exhibit collective expression level changes associated with HPT1 adenoma development. miRNAs, predicted *in silico* to target these genes, did not exhibit a clear tendency upon experimental validation.

Conclusions: The presented gene expression analysis provides a differential molecular characterization of PG adenoma and hyperplasia pathologies, advancing our understanding of their etiology. **(*J Clin Endocrinol Metab* 103: 2189–2198, 2018)**

ISSN Print 0021-972X ISSN Online 1945-7197
Printed in USA

Received 19 November 2017. Accepted 2 April 2018.
First Published Online 5 April 2018

Abbreviations: FFPE, formalin-fixed paraffin-embedded; HPT1, primary hyperparathyroidism; HPT2, secondary hyperparathyroidism; MEN1, menin 1; miRNA, microRNA; mRNA, messenger RNA; PG, parathyroid gland; PTH, parathyroid hormone; RT-qPCR, reverse transcription quantitative polymerase chain reaction; VDR, vitamin D (1,25-dihydroxyvitamin D3) receptor.

Hyperparathyroidism (HPT) is characterized by the oversecretion of parathyroid hormone (PTH). Primary HPT (HPT1) is a dysfunction of the parathyroid tissue with autonomous over-secretion and unclear etiology, leading to high serum calcium level, whereas secondary HPT (HPT2) generally results from hypocalcemia and/or low vitamin D level (1). HPT1 has a prevalence of 3:1000 in the general population (2). Most HPT1 cases are sporadic, with only 5% being hereditary, including multiple endocrine neoplasia [MEN1 (*MEN1 tumor suppressor*), MEN2A (*RET proto-oncogene*), MEN4, hyperparathyroidism-jaw tumor syndrome (*HRPT2*), and familial hypocalciuric hypercalcemia, *CaSR*] (1). HPT1 is caused by a single gland adenoma in 80% to 85% of cases, diffuse hyperplasia of all four glands in 12% to 15% of cases, or double adenomas in 2% to 5%. Parathyroid carcinoma is extremely rare (<1%). Histologically, parathyroid tumors are heterogeneous, with subtle differences between histologic subtypes, making classifications difficult. Studies of clonality did not allow distinguishing between these tumor types (3), and their diagnosis remains challenging.

Somatic alterations in *MEN1* and cyclin D1 genes have emerged as important drivers in the development of 25% to 40% of sporadic parathyroid adenomas (4). No somatic mutations of the *CaSR* gene have been identified in sporadic HPT so far, although its role in familial HPT is well documented (5). Reduced expression of vitamin D (1,25- dihydroxyvitamin D3) receptor *(VDR)* and *CaSR*, translating aberrant CaSR signaling, was detected in sporadic parathyroid adenomas, suggesting their role in parathyroid tumorigenesis (6). Moreover, mutation in tumor suppressor gene *HRPT2,* encoding for parafibromin protein, was detected in familial and sporadic parathyroid carcinoma (7).

Diurnal variation of PTH levels exhibit pronounced circadian rhythm, with peak levels in the early morning. When comparing patients with HPT1 with healthy subjects, the circadian rhythm of serum PTH level seems to be disrupted in patients with HPT1 with a return to rhythm for serum PTH observed only after surgical treatment of HPT1 (8). Moreover, circadian disruption is often associated with cell-cycle dysregulation and tumorigenesis (9–11). The changes in core-clock gene expression exhibit tissue and tumor specificity and have not yet been explored for the parathyroid gland (PG).

MicroRNAs (miRNAs) are conserved small noncoding RNA, functioning as negative regulators of gene expression (12). A large-scale study by Rahbari *et al.* (13) detected downregulation of most PG miRNAs in parathyroid carcinoma, with the upregulation of these miRNAs in HPT1.

In spite of substantial efforts, there are still no reliable molecular markers associated with histological HPT subtypes. To better understand the etiology of distinct PG pathologies, comparative large-scale transcript expression analysis by probe-based NanoString has been conducted in PG adenoma and hyperplasia. To get possible mechanistic insights into these obtained molecular patterns, *in silico* differential miRNA expression analyses and modeling of the PG adenoma and hyperplasia messenger RNA (mRNA)–miRNA network have been undertaken and were validated experimentally.

Materials and Methods

Study participants and PG tissue sampling

Formalin-fixed paraffin-embedded (FFPE) samples from human PG were obtained from the archives of the Pathology Department, Geneva University Hospital. Normal PG FFPE samples were selected from patients without hyperparathyroidism whose PG was removed inadvertently during the planned thyroid surgery. Adjacent normal PG samples for paired analyses were selected from same patients with sporadic HPT1 adenoma. Fresh samples from PG adenomas were obtained at surgery. Control tissue samples from healthy PG were either accidentally dissected at total thyroidectomy or dissected from the neighboring parathyroid adenoma tissue. Samples were washed in phosphate-buffered saline, snap-frozen in liquid nitrogen, and stored at −80°C. Histological sections from the same tissues were processed for the classification. Clinical characteristics of all the patients are summarized in Supplemental Table 1. The study protocol was approved by the local ethics committee (CER 2016-01384).

RNA extraction

For RNA extraction from FFPE samples, 3-μm-thick tissue sections were deparaffinized in xylol, proteins were digested overnight, and total RNA was subsequently extracted using the High Pure miRNA isolation kit (Roche) according to the manufacturer's instructions. Regarding snap-frozen PG samples, 10 mg of tissue was homogenized, and total RNA was extracted using the High Pure miRNA isolation kit according to manufacturer's protocol.

Gene expression quantification using NanoString nCounter

Twenty-nine candidate genes were selected for analysis, including genes involved in PG function, circadian clock, cell cycle, and apoptosis, based on our own previous studies (14, 15) and on literature search. Probes were designed and synthesized by NanoString nCounter Technologies (Supplemental Table 2). A total of 400 ng of RNA, extracted from the FFPE samples, were hybridized with multiplexed probes, as described previously (16). Background correction was made by subtracting from the raw counts the mean ± 2 standard deviation of counts obtained with negative controls. Values <1 were fixed to 1 to avoid negative values after log transformation. Then, counts for target genes were normalized with the geometric mean of five housekeeping

genes (*HPRT1*, *RPL13A*, *GAPDH*, β-2-microglobulin, and β-actin) selected as the most stable using the geNorm algorithm (17). Normalized data were log2 transformed for further analyses.

Assessment of mRNA expression in snap-frozen PG samples

Gene expression was assessed in the total RNA (200 ng per sample) using reverse transcription quantitative polymerase chain reaction (RT-qPCR), as previously described by us (18). The RT-qPCR primers are listed in Supplemental Table 3. Expression level of each target gene was normalized to the average expression of two housekeeping genes (ribosomal protein S9 and *HPRT1*).

Statistical analyses

For NanoString data, statistical analysis was carried out as described in detail in the Supplemental Materials. Pairwise Pearson correlation analysis was applied to test the correlation between gene expression data obtained by NanoString and by RT-qPCR analysis. Student unpaired two-tailed *t* test was applied to compare obtained data from normal and adenoma PG tissue gene and miRNA expression.

Modeling the PG adenoma and hyperplasia mRNA–miRNA network

Based on the differential expression analysis of miRNA by Rahbari *et al.* (13), we selected miRNA that were significantly upregulated (with a false discovery rate <0.05) in HPT1 adenoma and hyperplasia. For each miRNA of interest, the predicted targets were retrieved from several sources (DIANA-microT, ElMMo, miRBase, miRanda, miRDB, PicTar, PITA, and TargetScan) using the *MultiMir* R package (19). We filtered the retrieved interaction using our list of identified genes. The resulting network was visualized with Igraph (20), mapping the information of the log fold change between hyperplasia or adenoma vs control condition.

Results

NanoString analysis of transcript expression patterns in HPT1 adenoma, HPT1 hyperplasia, and HPT2 hyperplasia compared with healthy PG tissue

NanoString analysis of 29 candidate genes, listed in Supplemental Table 2, was conducted in 6 normal PG, 18 HPT1 adenoma, 12 HPT1 hyperplasia, and 6 HPT2 hyperplasia samples (see Supplemental Table 1 for patient characteristics). Of note, the proto-oncogenic transcripts *c-MET* and *MYC* were 5-fold downregulated in HTP1 adenoma (Table 1). *NFIL3*, encoding for a protein that represses expression of the core-clock components PER1 and PER2, was downregulated 4-fold in HTP1 adenoma (Table 1). Expression of *CDKN1B* gene encoding for cyclin-dependent kinase inhibitor 1B,

Table 1. Altered Transcript Expression in HPT1 Adenoma, HPT1 Hyperplasia, and HPT2 Hyperplasia FFPE Samples Compared With Independent Healthy PG Samples (N = 6) or Adjacent Normal PG Samples From the Same Patients (N = 5, Paired Analysis)

Gene	*P* Value	Fold Change	Total Number of Samples	Number of Samples With Expression Value >50 (Linear Scale)
HPT1 adenoma (N = 18) vs healthy (N = 6)				
c-MET	0.0012	−5.13	24	19
MYC	0.0006	−5.66	24	24
NFIL3	0.0484	−4.16	24	23
CDKN1B[a]	0.0349	1.58	24	24
CRY1[a]	0.0242	−1.71	24	24
CRY2[a]	0.0058	−1.81	24	24
PER2[a]	0.0259	−1.75	24	24
HPT1 hyperplasia (N = 12) vs healthy (N = 6)				
RET	0.0382	−13.56	18	13
HPT2 hyperplasia (N = 6) vs healthy (N = 6)				
NFIL3	0.0320	−6.71	12	11
VDR	0.0347	−7.47	12	11
CDKN1B[a]	0.0247	1.82	12	12
CRY2[a]	0.0413	−1.69	12	12
HPT1 adenoma vs adjacent normal (paired samples from N = 5 human individuals)				
c-MET	0.0201	−3.07	10	9
MYC	0.0109	−4.23	10	10
NFIL3	0.0056	−3.68	10	10
PER1	0.0154	−2.12	10	10
TIMP1	0.0242	−4.55	10	10
CASR[a]	0.0193	−1.60	10	10
CDH1[a]	0.0150	1.84	10	10
DBP[a]	0.0213	1.74	10	10
VDR[a]	0.0234	−1.79	10	10

[a] Altered transcripts with fold change between 1.5 and 2.

inhibiting cell-cycle progression, was upregulated, whereas expression of core-clock genes *CRY1*, *CRY2*, and *PER2* was downregulated 1.5- to 2-fold in these samples (Table 1). Moreover, *RET* transcript levels revealed a trend toward a 7-fold downregulation, which did not reach statistical significance, whereas *TIMP1* was downregulated 2-fold (Supplemental Table 4).

In HTP1 hyperplasia, *RET* exhibited a 13-fold downregulation (Table 1), whereas the cell-cycle–related gene *cyclin-dependent kinase 1* showed a nonsignificant trend toward a 4-fold downregulation (Supplemental Table 3). In HPT2 hyperplasia, 6-fold downregulation was observed for *NFIL3*, with 7-fold for *VDR* (Table 1). Similarly, to HPT1 adenoma, expression of *CRY2* transcript was 1.7-fold downregulated, whereas *CDKN1B* exhibited significant 1.8-fold upregulation (Table 1). *RET* levels were downregulated 12-fold, and *CaSR* showed a trend toward a 45-fold downregulation, although without statistical significance (Supplemental Table 4).

NanoString analysis of transcript expression patterns in HPT1 adenoma and adjacent normal PG samples from the same patients (paired samples)

To ensure that the observed differences in gene expression were stemming from PG pathology itself and not from interindividual genetic background differences in our cohort, we next analyzed a subgroup of HPT1 adenoma samples compared with adjacent normal PG obtained from the same five patients (Supplemental Table 1, group 2* and 3*). In good agreement with the results obtained for unpaired samples (Table 1, upper), the expression levels of *c-MET, MYC*, and *NFIL3* exhibited a 2- to 4-fold downregulation (Table 1, paired sample analysis, lower). Moreover, *TIMP1* and *PER1* were significantly downregulated (Table 1, lower. Lower (1.5- to 2-fold) statistically significant downregulation was observed for *CaSR* and *VDR* transcripts, whereas *DBP* and *CDH1* transcripts were upregulated (Table 1, lower). Finally, a trend for 7-fold downregulation in expression levels of *RET* was observed (Supplemental Table 5).

Comparing transcript expression patterns in HPT1 adenoma, HPT1 hyperplasia, and HPT2 hyperplasia with combined group of paired and independent healthy PG samples

Additionally, a comparison among HPT1 adenoma, HPT1 hyperplasia, and HPT2 hyperplasia samples with all normal PG samples enrolled in this study (Supplemental Table 1; groups 1 and 2; N = 11) has been conducted. The levels of *c-MET, MYC, TIMP1, RET,* and *NFIL3* were significantly downregulated 3- to 7-fold in HTP1 adenoma. Lower but significant downregulation was observed for *CRY2,* whereas *CDH1* was upregulated 1.9-fold (Table 2).

In HTP1 hyperplasia, a 14-fold downregulation of *RET* was observed (Table 2), along with a trend for 2.5- and 8-fold downregulation of *cyclin-dependent kinase 1* and *CaSR*, respectively (Supplemental Table 6). In HPT2 hyperplasia, expression levels of *VDR* and *NFIL3* levels were downregulated by a 5- to 7-fold, *RET* by 14-fold, and *CaSR* was as much as 53-fold downregulated (Table 2).

Alteration in gene expression levels between different HPT histological subtypes

Finally, gene expression comparison has been conducted across HPT pathologies. The expression levels of tumor suppressor *CDH1* were 2-fold downregulated in

Table 2. Altered Transcript Expression in HPT1 Adenoma, HPT1 Hyperplasia, and HPT2 Hyperplasia Samples Compared With All Healthy PG Samples and Adjacent Normal PG Samples (N = 11, Representing the Two Groups of Healthy Controls Presented in Table 1 Combined)

Gene	*P* Value	Fold Change	Total Number of Samples	Number of Samples With Expression Value >50
HPT1 adenoma vs combined control samples				
c-MET	0.0002	−4.33	29	24
MYC	0.0001	−4.82	29	29
NFIL3	0.0352	−3.25	29	28
RET	0.0265	−7.61	29	25
TIMP1	0.0199	−2.99	29	29
CDH1[a]	0.0383	1.92	29	29
CRY2[a]	0.0041	−1.61	29	29
HPT1 hyperplasia vs combined control samples				
RET	0.0077	−14.75	23	18
HPT2 hyperplasia vs combined control samples				
CaSR	0.0167	−53.09	17	15
NFIL3	0.0259	−5.24	17	16
RET	0.0296	−13.95	17	14
VDR	0.0115	−7.47	17	16

[a] Altered transcripts with fold change between 1.5 and 2.

HPT1 hyperplasia vs HPT1 adenoma, whereas *c-MET* and *MYC* levels were significantly upregulated (Table 3). To address differences in molecular pattern, 6 HPT2 hyperplasia and 18 HPT1 adenoma samples were compared. Transcript expression levels of *CDH1* and *CaSR* were downregulated 3- and 45-fold, respectively, whereas levels of *c-MET* and *MYC* were 3- to 4-fold upregulated (Table 3). When comparing transcriptional patterns of HPT2 vs HPT1 hyperplasia, no substantial alterations were revealed (Supplemental Table 7).

Alterations of c-MET, MYC, and NFIL3 expression levels in HPT1 adenoma exhibit pairwise correlations

As the NanoString approach assesses numerous transcript levels within the same sample, pairwise correlations have been established among the altered transcripts. In HPT1 adenoma, *c-MET* revealed strong positive correlations with *MYC* and *NFIL3* when compared with independent healthy PG samples (Fig. 1A), paired normal PG samples (Fig. 1B), and combined healthy samples (Fig. 1C). In summary, analysis of *c-MET, MYC*, and *NFIL3* levels in the same PG samples suggests that changes in the expression level of these genes is strongly correlated, which may indicate that collective changes in these gene expressions are tightly associated with HPT1 adenoma development.

miRNA–mRNA network in HPT1 adenoma and hyperplasia

Using the differential expression analysis of miRNA from Rahbari *et al.* (13), we selected miRNA that were significantly upregulated in HPT1 adenoma and at the same time were predicted to target the genes that were downregulated in our Nanostring analysis (Fig. 2). Indeed, miRNA (miR)-144-3p, miR-211-5p, miR-21-5p, and miR-218-5p were strongly upregulated in HPT1 adenoma and were predicted to target *c-MET* and *RET*. Additional upregulated miRNA were found to target *NFIL3, MYC*, and *TIMP1*, with some miRNA targeting multiple of these genes (Fig. 2; miR fold change in Supplemental Table 8). In HPT1 hyperplasia, miR-21-5p, miR-29b-3p, and miR-330-3p exhibited >1.5-fold change, and were predicted to target downregulated proto-oncogene *RET,* as well as *VDR* and *CaSR* (Supplemental Fig. 1; miR fold change in Supplemental Table 9).

Expression levels of the individual genes associated with PG pathologies and miRNA predicted to target these genes in snap-frozen PG samples

To validate the alterations in the gene expression observed in the studied PG pathologies employing NanoString analyses, we conducted qRT-PCR analyses on RNA extracted from snap-frozen healthy and adenoma PG tissues (see Supplemental Table 1 for patient clinical characteristics). In a good agreement with the NanoString results (Tables 1 and 2), significant 2- to 3-fold downregulation was observed for *c-MET*, *MYC*, and *CaSR* in this set of samples, whereas *TIMP1* was 1.87-fold down (Table 3). Of note, strong positive correlation between *c-MET* and *MYC* expression presented in Fig. 1 was confirmed in qRT-PCR data on snap-frozen samples (Table 3, $R = 0.67$, $P = 0.0469$). Finally, *PTH* expression was about 2-fold downregulated in the same PG adenomas.

Analysis of miRNA predicted to target these genes (Fig. 2), conducted in the same snap-frozen samples, revealed no substantial changes in the expression levels of miR-21-5p, miR-27a-3p, miR-34a-5p, miR-144-3p, and miR-218-5p between adenoma samples and healthy controls (Supplemental Table 10).

Discussion

NanoString analysis identifies c-MET, MYC, and NFIL3 as molecular markers associated with single HPT1 adenoma

NanoString nCounter is a color-coded probe-based method with a highly sensitive approach to quantification of gene expression. Based on direct probe hybridization, it allows for the collective assessment

Table 3. Altered Transcript Expression Between the Different HPT Subgroups

Gene	*P* Value	Fold Change	Total Number of Samples	Number of Samples With Expression Value >50
HPT1 hyperplasia vs HPT1 adenoma				
CDH1	0.0275	−2.06	30	30
c-MET	0.0110	2.69	30	25
MYC	0.0043	3.04	30	30
HPT2 hyperplasia vs HPT1 adenoma				
CaSR	0.0199	−45.32	24	22
CDH1	0.0063	−3.16	24	24
c-MET	0.0194	3.14	24	18
MYC	0.0045	4.05	24	24

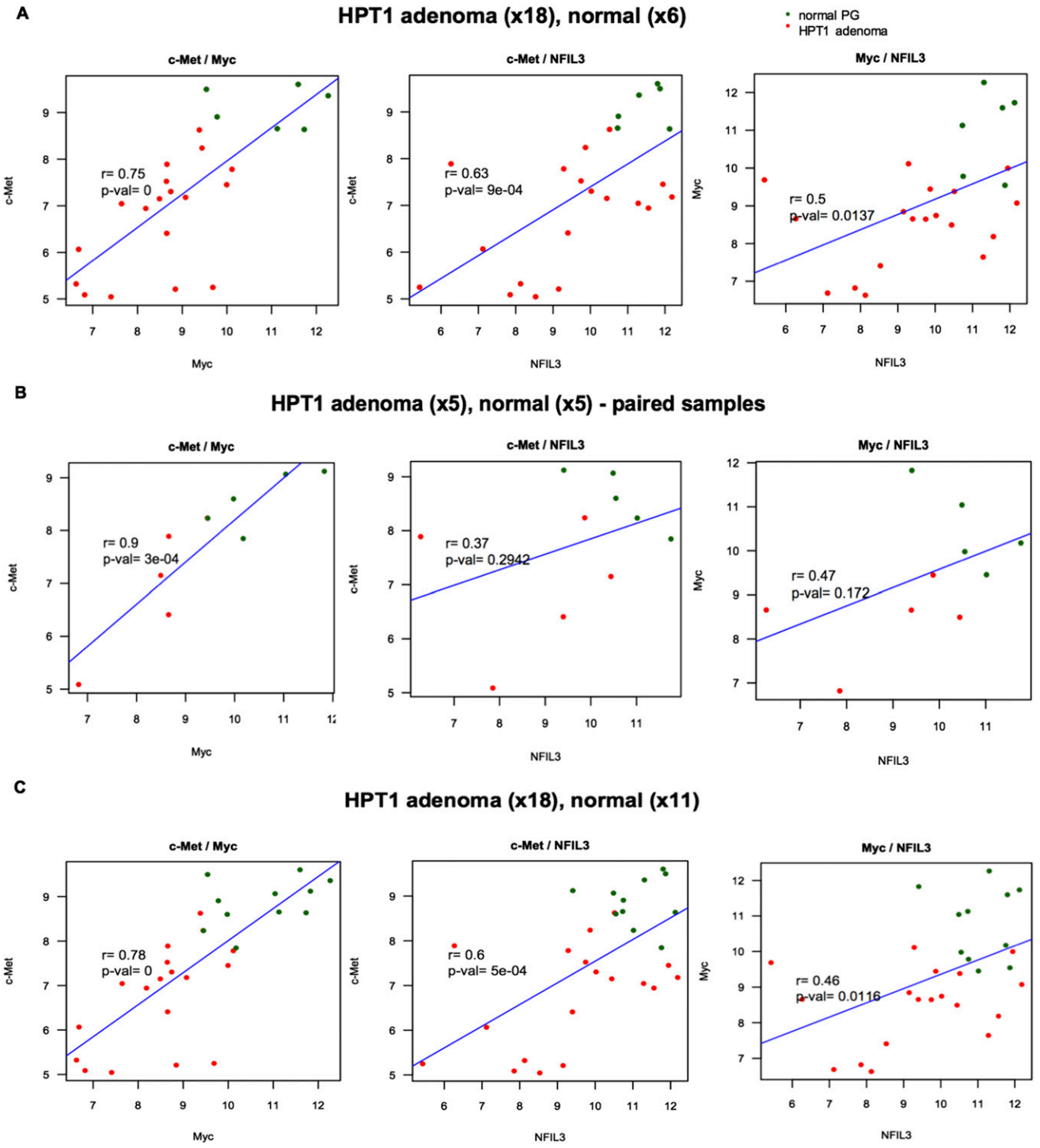

Figure 1. Pairwise correlations among *c-MET, MYC*, and *NFIL3* transcript changes in HPT1 adenoma. Pearson correlation analysis revealed pairwise correlations of transcript changes in HPT1 adenoma compared with (A) independent healthy PG samples, (B) paired PG samples and (C) combined healthy PG samples (n = 11). The correlation strength was based on Evans classification (see Methods), with a coefficient *r* value <0.20 reflecting very weak correlation; 0.20 to 0.39, weak; 0.40 to 0.59, moderate; 0.60 to 0.79, strong; and >0.80, very strong. The dots on each graph represent normalized respective gene expression values.

of a large number of transcripts within the same sample, including high precision analyses of FFPE samples, as previously demonstrated (14, 16). Using this powerful approach, we report important alterations of expression levels of *c-MET, MYC, TIMP1, CDH1*, and *NIFL3* in HPT1 adenoma (Tables 1 and 2), which was confirmed for *c-MET, MYC*, and *TIMP1* by qPCR analysis (Table 3). Importantly, screening of paired HPT1 adenoma and adjacent normal PG samples, attempting to rule out the possible bias introduced by interindividual differences, further validates that the observed transcriptional changes are likely to be associated with HPT1 adenoma development (Table 1).

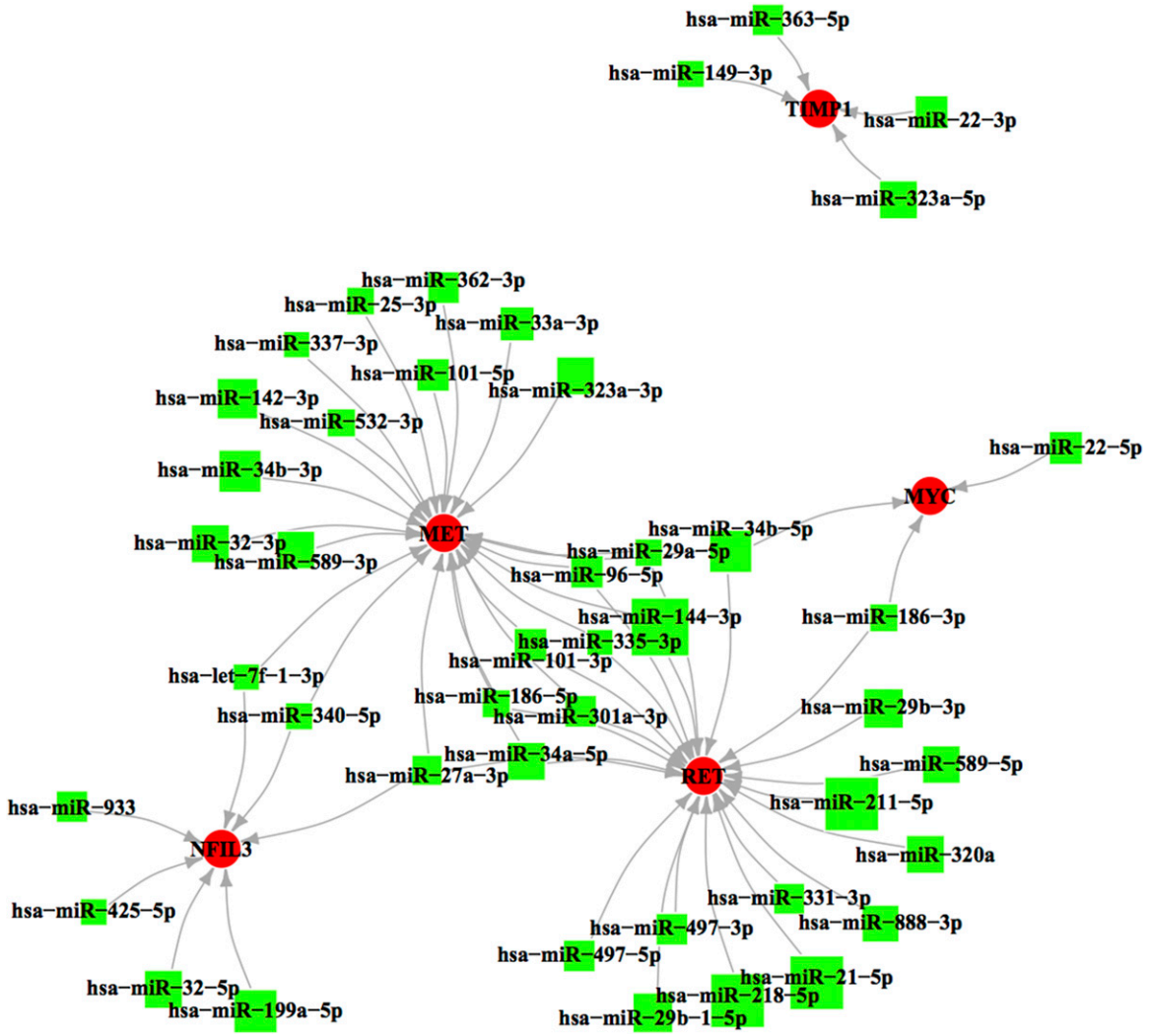

Figure 2. Network maps of miRNA in HPT1 adenoma. Network maps of upregulated miRNA based on log fold change between HPT1 adenoma vs control, using microarray data from Rahbari *et al.* (13). After retrieving the predicted targets for each miRNA, they were filtered based on the interactions using our list of differentially expressed biomarkers from the NanoString analysis. miRNA is represented with green cubes, with size according to log fold change; targeted genes are in red circles.

c-MYC, a well-characterized proto-oncogene involved in cell growth, differentiation, apoptosis, and invasion, was previously demonstrated to play a role in PG cell-cycle regulation (21). *c-MYC* mRNA has been previously shown to be overexpressed in a number of human cancers (14, 15), and in PG pathologies including HPT1 and HPT2 (22). A discrepancy between our data and previous work (22) may stem from the differences in the sample selection. Indeed, we separately assessed HPT1 hyperplasia and adenoma samples, which allowed us to distinguish hyperplasia from local changes associated with single adenoma. Moreover, MYC protein downregulation in subpopulation of cancer cells was reported to contribute to the cell survival upon glucose and oxygen deficiency (23), with glucose deprivation inducing MYC-mediated apoptosis in cancer cells (24). This may possibly explain the downregulation of *MYC* transcript observed by us in FFPE and snap-frozen adenomas (Tables 1 and 4).

Furthermore, although activation of c-MET and TIMP1, along with loss of function of CDH1, is associated with progression and metastasis in many of human cancers (25), our study demonstrates simultaneous downregulation of *c-MET*, *c-MYC*, and *TIMP1*, and upregulation of *CDH1* expression levels in HPT1

Table 4. Altered Transcript Expression Between Snap-Frozen HPT1 Adenoma (N = 5) and Healthy PG (N = 4) Samples

Gene	*P* Value	Fold Change
MET	0.013	−3.2
c-MYC	0.09	−2.27
TIMP1	0.078	−1.87
CaSR	0.005	−2.17

adenoma. Such differences in the gene transcription pattern may possibly represent a compensatory mechanism aiming at preventing further malignant transformation in this condition. Upregulation of *CDH1* was previously associated with sporadic PG carcinoma (26).

Analysis of HPT1 adenoma samples revealed strong pairwise correlations between *c-MET, MYC*, and *NFIL3* when compared with normal PG samples (Fig. 1). Specifically, *c-MET* and *MYC* transcript levels showed a strong positive correlation within the same FFPE and snap-frozen samples (Fig. 1). Furthermore, *NFIL3* transcript levels showed a strong positive correlation with those of *c-MET* and *MYC* within the same PG samples. These correlations, made possible by simultaneous analysis of these transcript levels in the same samples by the NanoString, strongly argue that the observed collective changes in these gene expressions might have functional significance, and further underscore a potential link between circadian clock and cell-cycle regulation during PG tumorigenesis.

Furthermore, in paired-sample analysis of HPT1 adenomas, a slight but statistically significant decrease in *CaSR* and *VDR* expression was observed (Table 1), in agreement with previous work reporting association of these genes with highly proliferative parathyroid adenomas (27). This finding was further confirmed for *CaSR* in snap-frozen adenomas (Table 4).

Finally, despite high PTH blood levels observed in patients with adenoma, *PTH* expression levels in HPT1 adenomas were downregulated (28), in a good agreement with our qRT-PCR data in snap-frozen adenomas.

miRNA may play a role in PG pathology development

One plausible mechanism for the observed downregulation of proto-oncogenes in PG pathologies could be through miRNA, because several have been shown to be upregulated in benign HPT1 but downregulated in parathyroid carcinoma (13). Indeed, miR-144-3p, miR-211-5p, miR-21-5p, and miR-218-5p, upregulated in HPT1 adenoma according to Rahbari (13), are targeting *c-MET*, *NFIL3*, *MYC*, and *TIMP1* according to our *in silico* analysis, with several miRs, comprising miR-27a-3p, miR34b-5p, and others targeting multiple genes (Fig. 2). Our qPCR analyses aimed to compare selected miRNA expression in adenoma and healthy snap-frozen PG samples revealed no substantial differences (Supplemental Table 10). This may most likely stem from high interindividual variability within each group and a low number of samples. Additional measurements of more PG samples will be required to draw firm conclusions regarding the potential role of miRNA in PG tumorigenesis.

NanoString analysis identifies circadian clock genes as molecular markers associated with HPT1 adenoma

Our NanoString analysis demonstrates reduced expression levels of core-clock genes *PER1, PER2, CRY1*, and *CRY2,* and clock output gene *NFIL3/E4BP4,* paralleled with upregulation of *DBP* in HPT1 adenoma, but not in hyperplasia (Tables 1 and 2). Disruption of circadian rhythms and changes in expression levels of individual core-clock genes have been previously linked to tumorigenesis (9–11). The circadian clock output gene *NFIL3/E4BP4* is a D-box–negative regulator that plays an essential role in setting the circadian period length of the mammalian oscillator, along with its positive D-box–regulating counterpart *Dbp* (29), in a good agreement with the opposite tendency that we observed for these gene alterations in paired HPT1 adenoma (Table 1). In view of the variable surgery timing, which makes the comparison of circadian gene levels between the samples problematic, the subgroup of paired samples (Table 1, lower) allows unbiased comparison of the clock gene expression.

A decrease in *PER1* expression level, observed by us in paired adenoma samples as well (Table 1), was previously reported in a variety of cancers, and loss of its rhythmic expression have been recently detected in human cholangiocarcinoma cells (30). Of note, miR-34a was also rhythmically expressed, and was directly targeting *PER1* in cholangiocarcinoma (30). Interestingly, according to our *in silico* analysis, miR-34a targets *PER1* (not shown) and *NFIL3* (Fig. 2), suggesting a potential link between overexpression of miR-34a and downregulation of *PER1* and *NFIL3*in HPT1 adenoma development. Our analysis of miR-34a expression in frozen samples failed to confirm this hypothesis (Supplemental Table 1), possibly because of the circadian variability of miR-34a expression, which may further increase the variability between subjects.

Altered gene expression in HPT hyperplasia identifies and confirms previously reported gene expression changes

Our analysis shows a strong downregulation of proto-oncogene *RET* expression in sporadic HPT1 and HPT2 hyperplasia (Tables 1 and 2). In contrast to MEN2-A, associated with oncogenic activation of RET tyrosine kinase domain (31), we have shown that sporadic HPT1 hyperplasia is associated with a decrease in *RET* expression, making this gene an excellent candidate for allowing to distinguish these two pathologies.

Importantly, our analysis reports an upregulation of *CDKN1B* gene in HPT2 hyperplasia and in HPT1 adenoma. It was recently shown that mutations in this gene

were associated with sporadic parathyroid adenomas (32). Also, we confirm a significant downregulation of expression of *CaSR* (as much as 54-fold) and *VDR* (7-fold) in HPT2 hyperplasia (Tables 1 and 2). This is consistent with previous studies reporting that sporadic parathyroid adenomas show reduced expression of *VDR* and *CaSR*, translating aberrant CaSR signaling, and both may play an important role in parathyroid tumorigenesis (6, 33). We report here a downregulation of circadian rhythm regulator, *NFIL3,* in HPT2 hyperplasia.

In summary, our study reveals that expression levels of *RET* and *NFIL3* genes are downregulated in HPT hyperplasia and confirms previously observed alterations in *CaSR* and *VDR* to be associated with this pathology.

Molecular distinction between PG hyperplasia and adenoma

Our comparative analysis between HPT adenoma and hyperplasia demonstrates significantly lower expression levels of *CDH1,* whereas *c-MET* and *MYC* transcripts showed significantly higher expression levels in both HPT1 and HPT2 hyperplasia compared with HPT1 adenoma (Table 4). Downregulation of *c-MET* and *MYC* in HPT adenoma vs hyperplasia might indicate a separate tumorigenesis pathway for adenoma. Studies have shown *MYC* expression to depend on calcium concentration and *CaSR* and to influence differentiation (34). Our findings may suggest that *CaSR* and *MYC* dysregulation is implicated in PG tumorigenesis. Furthermore, *CaSR* is significantly downregulated in HPT2 hyperplasia vs HPT1 adenoma, in agreement with previous studies (33), further confirming previous findings on aberrant CaSR signaling in hyperplasia. Similarly, our results confirm a downregulation of *VDR* in HPT2 hyperplasia in agreement with previous study (35).

In conclusion, this study provides a transcriptional characterization of healthy PG, sporadic HPT1 adenoma and hyperplasia, and HPT2 hyperplasia. Alterations of proto-oncogenes *c-MET, MYC,* and *TIMP1* and core-clock genes *NFIL3* and *PER1* were associated with PG adenoma. Additional transcripts related to PG function such as *CaSR* and *VDR* were significantly downregulated in HPT1 adenoma and HPT2 hyperplasia. Last, pairwise expression levels of *c-MET, MYC*, and *NFIL3* represent a cluster of markers whose collective changes are associated with HPT1 adenoma development and might be potentially predictive of HPT1 adenoma diagnosis. Observed collective changes in several transcripts involved in PG function, cell cycle, and circadian clock may suggest a functional importance for these expression changes.

Acknowledgments

The authors thank Mylene Docquier and Didier Chollet from the iGE3 Genomics Platform of the University of Geneva for performing NanoString analysis and Margaret Bercy from pathology for handling the FFPE tissue-blocks.

Financial Support: This work was funded by the Department of Surgery Research Grant (to S.M.S.) and the Fondation pour la Recherche sur le Cancer et la Biologie and Fonds de Recherche du Département des Spécialités de Médecine (to C.D.).

Author Contributions: S.M.S., M.P., M.-C.B.-M., V.P., C.D.V., J.S., C.D.-V., R.R., J.P., and F.T. contributed to data acquisition and analysis; E.K. provided microarray data; S.M.S. and C.D. designed the study and drafted the manuscript. All authors took part in the revision of the manuscript and approved the final version.

Correspondence and Reprint Requests: Samira Mercedes Sadowski, MD, Endocrine Surgery, Thoracic and Endocrine Surgery, University Hospitals of Geneva, Rue Gabrielle Perret-Gentil 4, 1211 Geneva 14, Switzerland. E-mail: Samira.Sadowski@hcuge.ch; or Charna Dibner, PhD, PD, Division of Endocrinology, Diabetes, Hypertension and Nutrition, Department of Internal Medicine Specialties, Faculty of Medicine and University Hospital of Geneva, Rue Michel-Servet, 1, 1211 Geneva 4, Switzerland. E-mail: Charna.Dibner@hcuge.ch.

Disclosure Summary: The authors have nothing to disclose.

References

1. Marcocci C, Cetani F. Clinical practice. Primary hyperparathyroidism. *N Engl J Med*. 2011;**365**(25):2389–2397.
2. Irvin GL III, Carneiro DM, Solorzano CC. Progress in the operative management of sporadic primary hyperparathyroidism over 34 years. *Ann Surg*. 2004;**239**(5):704–708, discussion 708–711.
3. Shi Y, Hogue J, Dixit D, Koh J, Olson JA Jr. Functional and genetic studies of isolated cells from parathyroid tumors reveal the complex pathogenesis of parathyroid neoplasia. *Proc Natl Acad Sci USA*. 2014;**111**(8):3092–3097.
4. Segiet OA, Deska M, Michalski M, Gawrychowski J, Wojnicz R. Molecular profiling in primary hyperparathyroidism. *Head Neck*. 2015;**37**(2):299–307.
5. Costa-Guda J, Arnold A. Genetic and epigenetic changes in sporadic endocrine tumors: parathyroid tumors. *Mol Cell Endocrinol*. 2014;**386**(1-2):46–54.
6. Sulaiman L, Juhlin CC, Nilsson IL, Fotouhi O, Larsson C, Hashemi J. Global and gene-specific promoter methylation analysis in primary hyperparathyroidism. *Epigenetics*. 2013;**8**(6):646–655.
7. Howell VM, Haven CJ, Kahnoski K, Khoo SK, Petillo D, Chen J, Fleuren GJ, Robinson BG, Delbridge LW, Philips J, Nelson AE, Krause U, Hammje K, Dralle H, Hoang-Vu C, Gimm O, Marsh DJ, Morreau H, Teh BT. HRPT2 mutations are associated with malignancy in sporadic parathyroid tumours. *J Med Genet*. 2003;**40**(9):657–663.
8. Logue FC, Fraser WD, Gallacher SJ, Cameron DA, O'Reilly DS, Beastall GH, Patel U, Boyle IT. The loss of circadian rhythm for intact parathyroid hormone and nephrogenous cyclic AMP in patients with primary hyperparathyroidism. *Clin Endocrinol (Oxf)*. 1990;**32**(4):475–483.
9. Dibner C, Sadowski SM, Triponez F, Philippe J. The search for preoperative biomarkers for thyroid carcinoma: application of the thyroid circadian clock properties. *Biomarkers Med*. 2017;**11**(3):285–293.
10. Mannic T, Meyer P, Triponez F, Pusztaszeri M, Le Martelot G, Mariani O, Schmitter D, Sage D, Philippe J, Dibner C. Circadian clock characteristics are altered in human thyroid malignant nodules. *J Clin Endocrinol Metab*. 2013;**98**(11):4446–4456.
11. Philippe J, Dibner C. Thyroid circadian timing: roles in physiology and thyroid malignancies. *J Biol Rhythms*. 2015;**30**(2):76–83.

12. Schickel R, Boyerinas B, Park SM, Peter ME. MicroRNAs: key players in the immune system, differentiation, tumorigenesis and cell death. *Oncogene*. 2008;**27**(45):5959–5974.
13. Rahbari R, Holloway AK, He M, Khanafshar E, Clark OH, Kebebew E. Identification of differentially expressed microRNA in parathyroid tumors. *Ann Surg Oncol*. 2011;**18**(4):1158–1165.
14. Chitikova Z, Pusztaszeri M, Makhlouf AM, Berczy M, Delucinge-Vivier C, Triponez F, Meyer P, Philippe J, Dibner C. Identification of new biomarkers for human papillary thyroid carcinoma employing NanoString analysis. *Oncotarget*. 2015;**6**(13):10978–10993.
15. Makhlouf AM, Chitikova Z, Pusztaszeri M, Berczy M, Delucinge-Vivier C, Triponez F, Meyer P, Philippe J, Dibner C. Identification of CHEK1, SLC26A4, c-KIT, TPO and TG as new biomarkers for human follicular thyroid carcinoma. *Oncotarget*. 2016;**7**(29):45776–45788.
16. Geiss GK, Bumgarner RE, Birditt B, Dahl T, Dowidar N, Dunaway DL, Fell HP, Ferree S, George RD, Grogan T, James JJ, Maysuria M, Mitton JD, Oliveri P, Osborn JL, Peng T, Ratcliffe AL, Webster PJ, Davidson EH, Hood L, Dimitrov K. Direct multiplexed measurement of gene expression with color-coded probe pairs [published correction appears in *Nat Biotechnol*. 2008;26:709]. *Nat Biotechnol*. 2008;**26**(3):317–325.
17. Vandesompele J, De Preter K, Pattyn F, Poppe B, Van Roy N, De Paepe A, Speleman F. Accurate normalization of real-time quantitative RT-PCR data by geometric averaging of multiple internal control genes. *Genome Biol*. 2002;**3**(7):RESEARCH0034.
18. Petrenko V, Saini C, Giovannoni L, Gobet C, Sage D, Unser M, Heddad Masson M, Gu G, Bosco D, Gachon F, Philippe J, Dibner C. Pancreatic α- and β-cellular clocks have distinct molecular properties and impact on islet hormone secretion and gene expression. *Genes Dev*. 2017;**31**(4):383–398.
19. Ru Y, Kechris KJ, Tabakoff B, Hoffman P, Radcliffe RA, Bowler R, Mahaffey S, Rossi S, Calin GA, Bemis L, Theodorescu D. The multiMiR R package and database: integration of microRNA-target interactions along with their disease and drug associations. *Nucleic Acids Res*. 2014;**42**(17):e133.
20. Csardi G, Nepusz T. The igraph software package for complex network research. InterJournal *Complex Syst*. 1695;**2006**(5):1–9.
21. Kremer R, Bolivar I, Goltzman D, Hendy GN. Influence of calcium and 1,25-dihydroxycholecalciferol on proliferation and proto-oncogene expression in primary cultures of bovine parathyroid cells. *Endocrinology*. 1989;**125**(2):935–941.
22. Björklund P, Akerström G, Westin G. Accumulation of non-phosphorylated beta-catenin and c-myc in primary and uremic secondary hyperparathyroid tumors. *J Clin Endocrinol Metab*. 2007;**92**(1):338–344.
23. Okuyama H, Endo H, Akashika T, Kato K, Inoue M. Down-regulation of c-MYC protein levels contributes to cancer cell survival under dual deficiency of oxygen and glucose. *Cancer Res*. 2010;**70**(24):10213–10223.
24. Shim H, Chun YS, Lewis BC, Dang CV. A unique glucose-dependent apoptotic pathway induced by c-Myc. *Proc Natl Acad Sci USA*. 1998;**95**(4):1511–1516.
25. Beavon IR. The E-cadherin-catenin complex in tumour metastasis: structure, function and regulation. *Eur J Cancer*. 2000;**36**(13 Spec No):1607–1620.
26. Haven CJ, Howell VM, Eilers PH, Dunne R, Takahashi M, van Puijenbroek M, Furge K, Kievit J, Tan MH, Fleuren GJ, Robinson BG, Delbridge LW, Philips J, Nelson AE, Krause U, Dralle H, Hoang-Vu C, Gimm O, Morreau H, Marsh DJ, Teh BT. Gene expression of parathyroid tumors: molecular subclassification and identification of the potential malignant phenotype. *Cancer Res*. 2004;**64**(20):7405–7411.
27. Yano S, Sugimoto T, Tsukamoto T, Chihara K, Kobayashi A, Kitazawa S, Maeda S, Kitazawa R. Decrease in vitamin D receptor and calcium-sensing receptor in highly proliferative parathyroid adenomas. *Eur J Endocrinol*. 2003;**148**(4):403–411.
28. Haglund F, Juhlin CC, Kiss NB, Larsson C, Nilsson IL, Höög A. Diffuse parathyroid hormone expression in parathyroid tumors argues against important functional tumor subclones. *Eur J Endocrinol*. 2016;**174**(5):583–590.
29. Yamajuku D, Shibata Y, Kitazawa M, Katakura T, Urata H, Kojima T, Takayasu S, Nakata O, Hashimoto S. Cellular DBP and E4BP4 proteins are critical for determining the period length of the circadian oscillator. *FEBS Lett*. 2011;**585**(14):2217–2222.
30. Han Y, Meng F, Venter J, Wu N, Wan Y, Standeford H, Francis H, Meininger C, Greene J Jr, Trzeciakowski JP, Ehrlich L, Glaser S, Alpini G. miR-34a-dependent overexpression of Per1 decreases cholangiocarcinoma growth. *J Hepatol*. 2016;**64**(6):1295–1304.
31. de Groot JW, Links TP, Plukker JT, Lips CJ, Hofstra RM. RET as a diagnostic and therapeutic target in sporadic and hereditary endocrine tumors. *Endocr Rev*. 2006;**27**(5):535–560.
32. Costa-Guda J, Marinoni I, Molatore S, Pellegata NS, Arnold A. Somatic mutation and germline sequence abnormalities in CDKN1B, encoding p27Kip1, in sporadic parathyroid adenomas. *J Clin Endocrinol Metab*. 2011;**96**(4):E701–E706.
33. Farnebo F, Enberg U, Grimelius L, Bäckdahl M, Schalling M, Larsson C, Farnebo LO. Tumor-specific decreased expression of calcium sensing receptor messenger ribonucleic acid in sporadic primary hyperparathyroidism. *J Clin Endocrinol Metab*. 1997;**82**(10):3481–3486.
34. Raffeiner P, Schraffl A, Schwarz T, Röck R, Ledolter K, Hartl M, Konrat R, Stefan E, Bister K. Calcium-dependent binding of Myc to calmodulin. *Oncotarget*. 2017;**8**(2):3327–3343.
35. Carling T, Rastad J, Szabó E, Westin G, Akerström G. Reduced parathyroid vitamin D receptor messenger ribonucleic acid levels in primary and secondary hyperparathyroidism. *J Clin Endocrinol Metab*. 2000;**85**(5):2000–2003.